Published in final edited form as:

Mucosal Immunol. 2018 May ; 11(3): 741–751. doi:10.1038/mi.2017.117.

Noxa/HSP27 Complex Delays Degradation of Ubiquitylated IkBα in Airway Epithelial Cells to Reduce Pulmonary Inflammation

Chunyu Zhang[1,6,*], **Jane T. Jones**[1,*], **Hitendra S. Chand**[1,7], **Marc G. Wathelet**[2], **Christopher M. Evans**[3], **Burton Dickey**[4], **Jialing Xiang**[5], **Yohannes A. Mebratu**[1], and **Yohannes Tesfaigzi**[1]

[1]COPD Program, Lovelace Respiratory Research Institute, Albuquerque, NM 87108, USA

[2]Infectious Diseases Program, Lovelace Respiratory Research Institute, Albuquerque, NM 87108, USA

[3]Pulmonary Sciences and Critical Care Medicine, University of Colorado, CO 80045, USA

[4]Division of Internal Medicine, The University of Texas M. D. Anderson Cancer Center, Houston, TX, 77030, USA

[5]Department of Biological and Chemical Sciences, Illinois Institute of Technology, Chicago, IL 60616, USA

Abstract

IFN-γ is known as a pro-inflammatory cytokine, but can also block inflammation in certain chronic diseases although the underlying mechanisms are poorly understood. We found that IFN-γ rapidly induced Noxa expression and that extent of inflammation by repeated house dust mite exposure was enhanced in *noxa*$^{-/-}$ compared with *noxa*$^{+/+}$ mice. Noxa expression blocked TNF-α-induced nuclear translocation of NF-κB and the production of pro-inflammatory cytokines. Noxa did not affect TNF-α-induced IκBα phosphorylation but the degradation of 48-chain-ubiquitylated IκBα. The Cys25 of Noxa was cross-linked with Cys137 of phospho-HSP27 and both proteins were required for blocking the degradation of ubiquitylated IκBα. Because, phospho-HSP27 is present in airway epithelial cells and not in fibroblasts or thymocytes, we generated transgenic mice that inducibly expressed Noxa in airway epithelia. These mice showed protection from allergen-induced inflammation and mucous cell metaplasia by blocking nuclear translocation of NF-κB. Further, we identified a Noxa-derived peptide that prolonged degradation of 48-chain-ubiquitylated IκBα blocked nuclear translocation of NF-κB, and reduced allergen-induced

Corresponding author: Yohannes Tesfaigzi, Lovelace Respiratory Research Institute, 2425 Ridgecrest Dr. SE, Albuquerque, NM 87108, Tel: (505) 348-9495, Fax: (505) 348-8567, ytesfaig@lrri.org.

[6]Present address: Department of Oncology, Johns Hopkins Bayview Medical Center, Baltimore, MD 21224, USA

[7]Present address: Department of Immunology, Herbert Wertheim College of Medicine, Florida International University Miami, FL 33199, USA

*These authors contributed equally.

Author Contributions: CZ performed most of the experiments and drafted parts of the paper, JJ conducted the peptide, HDM, and ubiquitylation studies, HC performed the immunofluorescence studies, MW provided strategies to generate various mutation constructs, JX propagated the adenoviral constructs, YM helped with the mouse studies, YT designed the studies and wrote the manuscript for review by all co-authors.

Disclosure/Conflict of Interest: The authors have no conflicting financial interests.

inflammation in mice. These results suggest that the anti-inflammatory role of the Noxa protein may be restricted to airway epithelial cells and the use of Noxa for therapy of chronic lung diseases may be associated with reduced side effects.

Introduction

IFN-γ is primarily produced by innate cells, including natural killer (NK) and natural killer T (NKT) cells, non-cytotoxic innate lymphoid cells [1], and adaptive immune cells, including $CD4^+$ T helper (Th) 1 and $CD8^+$ cytotoxic T lymphocytes (CTL) cells. [2] IFN-γ activates macrophages to produce pro-inflammatory cytokines[3], but can also counteract inflammatory and immunostimulatory pathways[4]. Transgenic mice engineered to express IFN-γ in airway epithelial cells were found to present with increased inflammation and emphysema[5] but also with reduced eosinophilia and airway reactivity[6]. However, because airway epithelial cells do not express IFN-γ the findings in these transgenic mice may not be physiologically relevant.

For clinical applications, IFN-γ has beneficial effects when administered as prophylactic treatment of lupus nephritis[7] and in cases of rheumatoid arthritis.[8] IFN-γ signaling inhibits neutrophil accumulation in the lung[9] or suppresses neutrophil production in the bone marrow.[10] These anti-inflammatory responses are mediated by induction of cytokine decoy receptors, IL-1Rα and IL-18BP.[2] Further, IFN-γ tempers the development of erythrocytes and eosinophilic granulocytes [11], and inhibits Th2 cell function. [12]

Because chronic inflammation promotes chronic lung diseases[13], identifying the intracellular factors that mediate the anti-inflammatory action of IFN-γ can be of great importance. Our previous studies have shown that IFN-γ causes cell death in airway epithelial cells by activating STAT1[14], inducing expression of the BH3-only protein, Bik[15], and suppression of Bmf expression to induce autophagy.[16] Bik and Bmf are Bcl-2 family members that share only the Bcl-2 homology region 3 (BH3) such as Noxa, Puma, Bim, Bid, Bad, Bid, Bnip-3L, and Hrk. This group of proteins is believed to sense cell death signals that emanate from internal stresses such as DNA damage[17] or CAP-independent translation[18] or from external stimuli, such as IFN-γ[15] or other cytokines.[19]

We found that in airway epithelial cells IFN-γ dramatically induced the BH3-only protein, Noxa, but that Noxa did not induce cell death, yet inhibited inflammation in response to allergen. Noxa required the interaction with phosphorylated HSP27 via a covalent disulfide bond to suppress the nuclear translocation and activation of NF-κB by inhibiting degradation of ubiquitylated κBa. Furthermore, inducible expression of Noxa in airway epithelia of adult mice suppressed allergen-induced inflammation *in vivo*. However, the cross-linking Cys25 was not necessary when the N-terminal peptide was used to block IκBα degradation and inflammation. Therefore, these studies identify the anti-inflammatory mediator of IFN-γ to be Noxa cross-linked to the non-Bcl-2 protein, pHSP27 that renders N-terminal region of Noxa functional.

Results

IFN-γ rapidly induces Noxa expression to suppress inflammation

Noxa mRNA levels were dramatically induced by 25-50 ng/ml IFN-γ treatment over 24-48 h in primary HAECs from non-diseased individuals (Fig. S1A). Induction occurred within 1 h of IFN-γ treatment both for Noxa mRNA (Fig. 1A), and protein levels (Fig. 1B), while Hrk, Bad, or Puma showed no change in expression (data not shown). This rapid induction by IFN-γ was consistently observed in HAECs from 14 individuals (Fig. 1C). As expected, Noxa protein and mRNA were undetectable in MAECs from *noxa*$^{-/-}$ mice but Noxa expression was increased by IFN-γ in wild-type MAECs (Fig. S1B). IFN-γ failed to upregulate Noxa expression in MAECs from *STAT1*$^{-/-}$ mice (Fig. S1B). However, unlike the DNA damage-induced Noxa expression [20], IFN-γ-induced Noxa expression was independent of p53 (Fig. S1C).

Noxa deficiency causes increased inflammation

While Noxa mRNA and protein levels were induced robustly by IFN-γ, *noxa*$^{+/+}$ and *noxa*$^{-/-}$ airway cells were both susceptible to IFN-γ-induced cell death (Fig. S1D). However, we observed that *noxa*$^{-/-}$ compared with *noxa*$^{+/+}$ mice developed increased inflammation following intranasal instillation with house dust mite allergen for 5 consecutive days. The numbers of total cells (Fig. 1D) eosinophils and macrophage, but not neutrophils and lymphocytes (Fig. 1E) recovered by bronchoalveolar lavage (BAL) were significantly higher in *noxa*$^{-/-}$ compared with *noxa*$^{+/+}$ mice. In addition, when sensitized with ovalbumin (OVA) injection on days 1 and 7 and challenged with OVA aerosols for 5 d, mucous cell numbers were higher (Fig. S2A) and inflammatory cells were more evident in *noxa*$^{-/-}$ compared with *noxa*$^{+/+}$ mice (Fig. S2B). These observations suggested that Noxa may play a role in blocking allergen-induced inflammation, but not in the cell death process of hyperplastic airway epithelial cells. Previous studies have shown that Noxa expression sensitizes cells to apoptosis [21]. To determine whether Noxa sensitizes airway epithelial cells, we first treated HAECs with increasing H_2O_2 concentrations and found that 45 μM affects cell viability slightly (Fig. S2C). However, when combined with increasing multiplicity of infection (MOI) of Ad-Noxa, cell viability was progressively reduced compared to the Ad-GFP controls (Fig. S2D).

Because expression of many pro-inflammatory genes are regulated by NF-κB including IL-8,[22] we investigated whether Noxa suppresses the synthesis of inflammatory chemokines. The TNFα-induced IL-8 secretion from human airway epithelial cells was significantly reduced when Noxa was expressed using an adenoviral expression vector (Ad-Noxa) compared to Ad-GFP-infected controls (Fig. 2A). The possible role of Noxa in affecting NF-κB activation was tested using the A549-NF-κB-luc cells that are stably transfected with a luciferase reporter gene driven by a promoter containing several NF-κB response elements. As expected, TNFα-induced luciferase activity was inhibited when Noxa was expressed in a dose-dependent manner (Fig. 2B); no cell death was detected by Ad-Noxa even at a MOI of 300 (data not shown). Further, suppression of Noxa expression using shRNA enhanced IFN-γ-induced NF-κB activity in cells treated with TNFα for 30 min (Fig. 2C). Further, merely expressing Noxa or expressing Noxa in the presence of IFN-γ treatment showed a similar

reduction in A549-NF-κB-luc cells, showing that IFN-γ had no further impact on Noxa-mediated suppression of NF-κB activity (Fig. S2F). Together, these findings suggest that the anti-inflammatory effect of IFN-γ is mediated by Noxa. We next analyzed the effects of IFN-y or Noxa on TNFα-induced change in sub-cellular localization of NF-κB. While NF-κB was localized to the nucleus 30 min after TNFα treatment, it remained localized to the cytosol in cells that were pretreated with IFN-γ for 24 h (Fig. 2D). Similarly, direct expression of Noxa using adenoviral vectors suppressed TNFα-induced nuclear translocation of NF-κB as shown by immunofluorescence (Fig. 2E). In addition, IFN-γ was delayed in suppressing nuclear translocation of NF-κB in *noxa*$^{-/-}$ MAECs (Fig. 2F), confirming that IFN-γ requires Noxa to delay NF-κB activation. These findings were further confirmed by immunoblotting of nuclear and cytoplasmic extracts that showed nuclear NF-κB being significantly reduced in cells pretreated with IFN-γ compared to non-treated controls (Fig. S2F).

Noxa blocks the degradation of ubiquitylated IκB-α

In non-stimulated cells, the inhibitory IκBα protein sequesters NF-κB to the cytoplasm and inflammatory stimuli activate IKKα and IKKβ to phosphorylate IκBα, which leads to its ubiquitylation and proteasomal degradation, releasing NF-κB to translocate to the nucleus. [23, 24] Over 0, 15, and 30 min of TNFα treatment, IκBα levels were reduced in the cytosolic extracts of *noxa*$^{-/-}$ but not *noxa*$^{+/+}$ MAECs (Fig. S2G), suggesting that Noxa stabilizes IκBα. TNFα-induced nuclear translocation of NF-κB was also significantly reduced following overexpression of Noxa using Ad-Noxa compared to cells infected with Ad-GFP (Fig. 2G), suggesting that Noxa expression is sufficient to stabilize IκBα. Interestingly, after 10 min of TNF-α treatment the levels of phosphorylated IκBα were similar in HAECs infected with Ad-Noxa and Ad-GFP as control (Fig. 2H). Lysine-48 (K48)-linked polyubiquitin chains are well established as the canonical signal for proteasomal degradation [25]. Interestingly, the levels of IκBα with homotypic K48-linked ubiquitin chains were increased in HAECs infected with Ad-Noxa and expressed Noxa compared with Ad-GFP-infected controls (Fig. 2I). This finding suggests that Noxa blocks the proteasomal degradation of IκBα that is already destined for degradation.

Noxa is cross-linked to phosphorylated HSP27

Because Noxa is known to inactivate Mcl-1 and thereby sensitize cells to apoptotic death[26, 27] we tested the hypothesis that Noxa may interact with other protein(s) to gain anti-inflammatory properties. Noxa antibodies consistently detected a cross-reacting protein of approximately 32 kDa in size only in IFN-γ-treated HAECs (Fig. 3A). Peptide mass fingerprint analysis of the cross-reacting the 32 kDa band excised following immunoprecipitation repeatedly revealed a high score for HSP27 (Table S1). This observation was confirmed by immunoblotting of anti-Noxa immunoprecipitated proteins with an antibody to HSP27 phosphorylated at Ser_{82} (Fig. 3B). Interestingly, Mcl-1 and Bcl-x_L, proteins known to interact with Noxa, [27] were not detected in the immunoprecipitates (Fig. 3B). Immunoprecipitation with p-S_{82}HSP27 antibodies confirmed that Noxa forms a complex with phosphorylated HSP27 (pHSP27) (Fig. 3C). The interaction between Noxa and pHSP27 was further verified by pull-down assays from extracts prepared from AALEB cells using recombinant, purified GST-Noxa protein and detecting pHSP27 protein by

Western blot analysis (Fig. 3D). Blocking the phosphorylation of expressed HSP27 using the p38MAPK inhibitor, SB203580, reduced the levels of immunoprecipitated pHSP27-Noxa complex (Fig. 3E), further supporting that pHSP27 rather than total HSP27 needs to be present to form the Noxa/pHSP27 interaction. Interestingly, merely overexpressing Noxa by infecting cells with Ad-Noxa in the absence of IFN-γ also resulted in the appearance of the 32 kDa Noxa-pHSP27 complex (Fig. S3A), suggesting that IFN-γ was not inducing a cross linking enzyme to facilitate this complex formation. The idea that Noxa and p-HSP27 are linked by disulfide bond(s) was confirmed by the absence of the p-HSP27-GST-Noxa complex in pull-down products from cell extracts treated with the reducing reagent, DTT that cleaves disulfide bonds (Fig. S3B).

To identify the amino acids within Noxa that are responsible for the Noxa-HSP27 complex, we generated various mutant GST-Noxa proteins that were tested in pull-down assays. Deletions of 10 amino acids from the N-terminus (Noxa-Δ5′) or 14 amino acids from the C-terminus (Noxa-Δ3′), abrogated the interactions of Noxa and pHSP27 (Fig. S3C). Because 293T cells express no detectable levels of endogenous HSP27, these cells were co-transfected with an HSP27-expression vector along with wild-type Noxa, Noxa-2CS, and Noxa-3KR. Mutations of cysteines 25 and 51 to serines (Noxa-2CS) also disrupted the interactions while mutation of lysines 35, 38, and 41 to argnines (Noxa-3KR) did not (Fig. 3F). Further mutagenesis experiments demonstrated that only Cys_{25} residue was essential for the formation of Noxa-phospho-HSP27 complex (Fig. 3F) confirming the hypothesis that Noxa and HSP27 are linked by an intermolecular disulfide bond.

Because HSP27 contains only one cysteine residue at position 137, the role of this residue was investigated by comparing wild-type and C137A mutant HSP27 constructs expressed in 293T cells that were treated with IFN-γ to induce Noxa. Although expression levels of pHSP27 were equal in cells transfected with either construct, immunoprecipitation with Noxa antibodies showed that the formation of Noxa-pHSP27 was impaired in cells transfected with the C137A mutant and was accompanied by the loss of interactions with IκBα/NF-κB complex (Fig. 3G). These studies demonstrated that an intermolecular disulfide bond between Cys_{25} in Noxa and Cys_{137} in HSP27 cross-links Noxa to pHSP27 to allow the formation of a complex with IκBα and NF-κB.

HSP27 is essential for Noxa-κBα-NF-κB interaction

Suppression of HSP27 in AALEB cells by stably expressing shHSP27 did not affect IFN-γ-induced Noxa expression (Fig. S3D). These cells were used to investigate the contribution of pHSP27 in blocking nuclear translocation of NF-κB. As shown by immunofluorescence staining IFN-γ blocked nuclear translocation of NF-κB in shCtrl but not in shHSP27 cells (Fig. 3H). In addition, when Noxa or HSP27 expression in AALEB cells was reduced using shNoxa or shHSP27, IFN-γ no longer suppressed secretion of IL-8 (Fig. S3E) or IL-6 (Fig. S3F). Therefore, we proceeded to determine whether the interaction of Noxa with IκBα/NF-κB would be disrupted by reducing HSP27 levels. Although NF-κB and κBα were equally expressed in shCtrl and shHSP27 cells, the interactions between Noxa and NF-κB or κBα were abolished in shHSP27 cells (Fig. 3I). Immunoprecipitation with NF-κB (p65) antibodies from shHSP27 cell extracts showed that the interaction of NF-κB with IκBα was

essentially completely disrupted when cells were treated with TNFα, suggesting that IκBα degradation occurred faster when HSP27 was suppressed (Fig. 3I). Further, the NF-κB—Noxa interaction was disrupted in shHSP27 cells but not in shCtrl cells (Fig. 3I) and TNFα-induced degradation of IκBα was enhanced in shHSP27 compared with shCtrl cells (Fig. 3J), suggesting that pHSP27 also is crucial in stabilizing IκBα. Therefore, Noxa requires the presence of pHSP27 to interact with the IκBα/NF-κB complex and the cross-linking of pHSP27 and Noxa appears to play a critical role in stabilizing IκBα.

Inducible Expression of Noxa in AECs protects from allergic inflammation and mucous cell hyperplasia

Constitutive expression of HSP27 has been detected in the lungs of mice [28] but the presence phosphorylated HSP27 in various tissues and cell types have not been studied. Because the cross-linking of Noxa to pHSP27 may be specific to airway epithelia, we compared pHSP27 levels in various tissues and cell types. Phospho-HSP27 was detected in MAECs and in lung tissues but not in murine embryo fibroblasts, thymus, and liver tissues (Fig. 4A). To investigate the anti-inflammatory and possibly the therapeutic role of Noxa expression in airway epithelial cells *in vivo*, we generated a conditional inducible transgenic ($Noxa^{Ind}$) mouse using the tetO-CCSP promoter system. Immunofluorescence analyses showed induced levels of Noxa in the bronchial epithelial cells of three founder $Noxa^{Ind}$ mouse lines compared with wild-type littermates (Fig. 4B). These mice expressed Noxa mRNA and protein in the lung tissues 24 h post doxycycline (dox)-diet (Fig. 4C). These transgenic mice and littermate controls were instilled with house dust mite (HDM) extract for 5 consecutive days, given the dox-diet on days 6 and 7, and euthanized on day 8. The number of total inflammatory cells in the BAL fluid was reduced in $Noxa^{Ind}$ mice compared to littermate controls and these reduced numbers were due to reduced BAL eosinophils and lymphocytes (Fig. 4D). The no dox, no HDM, dox-fed but not HDM mice controls showed only macrophages and no inflammation (data not shown). Transgenic expression of Noxa also resulted in a 3-fold reduced number of mucous cells per mm basal lamina (BL) compared with littermate controls (Fig. 4E). Immunofluorescence analysis showed that expressed Noxa was co-localized with NF-κB in the cytosol resulting in the lower percentage of airway epithelial cells with nuclear NF-κB in $Noxa^{Ind}$ mice (Fig. 4F). Further, pHSP27 was co-localized with induced Noxa (Fig. S4A) and NF-κB (Fig. S4B) in airway epithelial cells of $Noxa^{Ind}$ mice.

The N-terminal Noxa peptide stabilizes IκBα and is anti-inflammatory

We further tested whether specific regions of the Noxa protein may act as anti-inflammatory by using Noxa-derived peptides. Based on our findings that Cys25 constitutes the cross-linking amino acid, and because the human and murine Noxa proteins share a high homology, except that the murine Noxa contains the duplicate sequence (Fig. S5A), we selected four regions that are 15 amino acids in length and span the following functional regions of the human Noxa protein. Peptide NoxaA represents the N-terminus, NoxaB contains Cys25, NoxaC comprises the BH3 domain, and NoxaD represents the C-terminal end of the protein (Fig. S5B). To facilitate uptake into cells, the peptides were synthesized with the HIV-derived TAT sequence on their N-termini. When A549 cells were treated with 10 ng/ml TNFα, NF-κB-induced luciferase activity, was reduced by NoxaA and NoxaD

peptides but not by NoxaB or NoxaC (Fig. 5A). However, when nuclear localization of NF-κB was investigated in TNFα-treated MAECs by immunofluorsence, only NoxaA but not NoxaD or the control TAT peptide affected nuclear localization (Fig. 5B).

To examine the anti-inflammatory effect *in vivo*, *noxa*$^{-/-}$ mice were intranasally instilled with 50 μg house dust mite allergen for 5 consecutive days and then instilled with NoxaA peptide on days 6 and 7. The number of inflammatory cells in the BAL fluid mice was significantly reduced by NoxaA (Fig. 5C) and this reduction was due to reduced numbers of eosinophils (Fig. 5D). The number of neutrophils, macrophages, and lymphocytes were not affected (data not shown). After 10 min of TNF-α treatment the levels of IκBα with homotypic K48-linked ubiquitin chains were increased in AALEB cells treated with NoxaA compared to Ctrl peptide (Fig. 5E).

Discussion

The present studies show that IFN-γ through STAT1 activation rapidly induces Noxa which is cross-linked with a non-Bcl-2 family member, pHSP27, and suppresses the canonical NF-κB signaling pathway. Therefore, these findings define the mediator by which IFN-γ acts as anti-inflammatory and are the first to show that a Bcl-2 family member could inhibit inflammation by reducing NF-κB activation.

Members of the extrinsic apoptotic machinery, including the TNFR1 interactors, TRADD, FADD, and RIPK1 [29] are known to be required for optimal NF-κB activation. The present study adds a new paradigm by showing that a member of the intrinsic apoptotic machinery affects the immune response by directly blocking NF-κB activation. It is well-established that proteins of the Bcl-2 family interact with each other to control the permeabilization of the mitochondrial outer membrane (MOM) and thereby regulate apoptosis. However, only a limited number of studies have explored their interaction with non-Bcl-2 family members and their roles in cellular processes other than those related to cell death. For example, Bad effects insulin secretion and metabolism [30] and BID, contrary to Noxa, by interacting with NOD1, NOD2, and the IκB kinase (IKK) complex facilitates NF-κB activation.[31]

Noxa is induced rapidly also by hypoxia via hypoxia-inducible factor (HIF)-1α[32] by DNA damage,[17] by ER stress inducing agents.[33] Furthermore, anticancer agents, including the proteasome inhibitor, bortezomib, or ubiquitylation of Mcl-1, induce Noxa expression.[35] All these studies used fibroblasts, chronic lymphocytic leukemia, melanoma, neuroblastoma, osteosarcoma, and lung cancer cells and investigated expressed Noxa interacting with the anti-apoptotic Mcl-1 to regulate cell death by affecting Mcl-1 degradation.[25,36] However, although Mcl-1 was present in airway epithelial cells, the presence of pHSP27 caused the IFN-γ-induced Noxa to prefer the cross-linking with pHSP27 and not Mcl-1. Ser_{13} phosphorylation alters Noxa structure and blocks the interaction site with Mcl-1.[34] Whether pHSP27 phosphorylates Noxa or just forces the N-terminal region to be exposed for interaction with IκBα is unclear. While the phosphorylation and ubiquitylation process remained unaffected, Noxa delayed the degradation IκBα after it was already tagged by the K48 ubiquitin chain. Small molecules, called ubistatins, block the binding of ubiquitylated substrates to the proteasome by targeting the ubiquitin-ubiquitin interface of K48-linked

chains.[35] Whether the N-terminus of Noxa interacts with the IκBα-specific proteins or the ubiquitin-ubiquitin interface or blocks the interaction of ubiquitylated IκBα to the 19S proteasome before being shuttled for degradation needs further investigation.

The airway epithelium is constantly exposed to the elements of the outer world and therefore has to continuously regulate inflammation. We show that Noxa is rapidly induced within hours and this rapid response allows the fine-tuning or unnecessary enhancement of inflammation. Given that Noxa expression in airway epithelium causes a significant difference in inflammation reveals that this protein contributes to the anti-inflammatory protective role of the airway epithelium. Because many pathways that are not necessarily associated with inflammation, including autophagy, regulators of ROS also play a role in regulating inflammation the induction of Noxa may be one of many mechanisms by which the airway epithelium dampens inflammation. Noxa expression can either sensitize airway cells when cells are damaged or inhibit inflammation. The present studies also suggest that the underlying mechanisms of Noxa-induced cell death in airway epithelial cells need further investigation, because Noxa-induced cell death may not only depend on enhanced degradation of Mcl-1 but also on blocking NF-κB activation that directly regulates expression of the anti-apoptotic Bcl-2.

Both the whole Noxa protein when cross-linked with pHSP27 and the peptide comprising the N-terminal region without the cross-linking Cys25 equally delayed the proteasomal degradation of ubiquitylated IκBα. Therefore, the role of pHSP27 is likely to expose the N-terminal region of Noxa to form a complex with IκBα and NF-κB. HSP27 has vastly different functions, including reducing growth or proliferation and increasing differentiation, and protecting against apoptosis.[36] This diverse function of HSP27 may depend on its ability as a chaperone protein to interact with other proteins that are present in various cell types or conditions. Further, HSP27 can be phosphorylated at three serine residues, resulting in the redistribution of the large oligomer into smaller tetrameric units, and its dephosphorylation favors the formation of large oligomers, the dimer of HSP27 being the building block for multimeric complexes that can be up to 1000 kDa.[37] It is possible that depending on the phosphorylation state, HSP27 interacts with different proteins to ultimately mediate different outcomes. For example, in prostate cancer cells, HSP27-eIF4E interaction defines the chaperoning role of HSP27 to decrease eIF4E ubiquitylation and proteasomal degradation to protect the protein synthesis initiation process and survival.[38] Similarly, hic-5 interacts with HSP27 and blocks the anti-apoptotic role of HSP27.[39]

Our finding that pHSP27 has an anti-inflammatory role is consistent with the report that HSP27 deficiency in mice augments neutrophil infiltration in wounds.[40] In other studies, HSP27 can enhance NF-κB activity by interacting with IKK [41] or by interacting with polyubiquitin chains.[42] However, these studies focused on analyzing the presence or absence of HSP27 and did not investigate the phosphorylation state of HSP27. Our studies demonstrate a novel observation that Noxa expression being highly induced in airway epithelial cells may define the anti-inflammatory function of pHSP27.

The finding that pHSP27 is primarily detected in lung tissues or airway epithelial cells would suggest that the anti-inflammatory role of Noxa is restricted to AECs. Consistent with

this hypothesis, inducible Noxa expression in airway epithelial cells of transgenic mice was effective in suppressing inflammation. Delivering the NoxaA peptide directly to the airways may be a useful tool to temper inflammatory responses by prolonging the half-life of IκBα. Therefore, developing therapeutic vectors that deliver Noxa proteins or peptides to the airway epithelium or molecules that specifically induce Noxa expression in airway cells would represent novel anti-inflammatory tools to control chronic inflammation. Noxa as treatment may be effective particularly in diseases that are associated with high levels of pHSP27, including COPD,[43] asthma,[44] and cancer.[45] IFN-γ has been used to treat chronic inflammatory diseases, but as a pleiotropic cytokine, it has many effects. By identifying Noxa as the protein that mediates the anti-inflammatory role of IFN-γ this study may have uncovered a means to harness the anti-inflammatory benefits of IFN-γ and minimize the other effects of IFN-γ This would place Noxa in a unique position among anti-inflammatory therapeutic agents, especially when prolonged treatments are expected in chronic inflammatory diseases, such as asthma and COPD.

Materials and Methods

Animals

All mouse studies were performed at the Lovelace Respiratory Research Institute (LRRI), a facility approved by the Association for the Assessment and Accreditation for Laboratory Animal Care International using protocols, pre-approved by the Institutional Animal Care and Use Committee (IACUC), and the Environmental Safety and Health department (ES&H). *Noxa*$^{-/-}$ on C57Bl/6 background mice were provided by Dr. A. Strasser (Walter and Eliza Hall Institute, Melbourne, Australia) and *p53*$^{-/+}$ breeders were purchased from The Jackson Laboratory (Ben Harbor, ME) and were bred at LRRI.[17] Mice were housed in isolated cages under specific pathogen-free conditions for the described studies.

The conditional and airway specific overexpression of Noxa was achieved by mating two lines of transgenic mice, the CCSP–reverse tetracyclineresponsive transactivator (rtTA) mice, bearing the rtTA under the control of the CCSP gene promoter (Perl et al 2009), and the tetracycline operator $(TetO)_7$–Noxa mice, containing TetO and minimal cytomegalovirus (CMV) promoter and the Noxa transgene. $(TetO)_7$-Noxa mice were generated at the M.D. Anderson Genetically Engineered Mouse Facility following standard methods and Institutional Animal Care and Use Committee-approved protocols and bred with CCSP-rtTA mice at LRRI. The transgene plasmid was cut with HindIII and NheI, and murine Noxa cDNA was separated from the TG-1 vector. Purified murine Noxa cDNA was injected into the pronuclei of zygotes collected from superovulated (C57BL/6) female mice, and injected zygotes were transferred to pseudopregnant ICR recipient females. Founder animals were identified by polymerase chain reaction amplification of 2.5 ul of tail DNA segments digested overnight in NaOH at 55°C. Oligonucleotides were as follows: a, 5′-AGGGATCCAT GTGTATTGTA TGTGGGCTC TAACCTGGC-3′ b, 5′-TGCAGCTAGG TGAGCGTCCA CAGGACCCTG AGTGGT-3′. To conditionally express murine Noxa in the lung, transgenic mice were fed with doxycycline-containing diet. Founder animals (C57Bl/6J) were bred to C57Bl/6J × C57Bl/6J animals to evaluate germline transmission. Six lines that transmitted the Noxa sequence were analyzed by q-PCR for expression of

Noxa in lung and tracheal tissue. On the basis of these results, three murine lines with expression of Noxa in the airway epithelia were chosen for colony expansion and line 2 was maintained by breeding with wild-type C57Bl/6 mice and using the wild-type littermates as controls for each experiment.

Exposures

At 6-10 weeks of age, mice were entered into the experimental protocols. Mice were instilled with HDM extracts for 5 consecutive days and lung tissues were analyzed 24 or 72 h post the last challenge. HDM (Greer Laboratories, Lenoir, NC) was from *Dermatophagoides Pteronyssinus*, (lot #248041), as 21.5 mg protein per 103.3 mg dry weight in a freeze-dried form, was resuspended in sterile phosphate buffered saline for a final concentration of 1μg/μl and stored in frozen aliquots at -20°C. Sensitization and exposure of mice to ovalbumin was as described previously.[46] Bronchoalveolar lavage and preparation of lung tissues for histopathological examination and staining with Alcian blue/ hematoxylin and eosin (H&E) was as described.[46]

Cells

Primary human airway epithelial cells (HAECs) (Cambrex Bio Science Walkersville, Inc.), murine airway epithelial cells (MAECs), AALEB cells, A549 cells stably transfected with multiple copies of the NF-κB response element driving a luciferase reporter construct (A549-NF-κB-luc cell line) (Panomics, Inc., CA.), and 293T cells were cultured as described previously.[14] AALEB cells are immortalized HAECs that have been well characterized [47]. Cells were maintained in bronchial epithelial growth medium BEGM (Lonza) supplemented with growth factors (BEGM Singlequots, Lonza) as described previously [14]. Adenoviral expression vectors for Noxa were provided by Dr. G. Shore (McGill University, Montreal, Canada), and cells were infected as previously described [48]. The A549-NF-κB-luc cell line was purchased from Panomics, Inc., CA. and grown in DMEM (Invitrogen) supplemented with 10% fetal bovine serum (FBS), 1mM sodium pyruvate, (Invitrogen), penicillin/streptomycin (Invitrogen) and hygromycin. The 293T cells were cultured in DMEM with 10% FBS. Transfections were carried out with the TransIT-2020 Transfection Reagent (Mirus Bio) according to manufacturer's protocol. Cell viability was determined by trypan blue exclusion.

Mouse airway epithelial cells (MAECs) were isolated essentially as described previously [49] by incubation in pronase solution (DMEM, 1.4 mg/ml pronase and 0.1 mg/ml DNase) overnight at 4°C to dissociate airway epithelial cells from the basal lamina. Cells were collected by gently rocking trachea in DMEM/Ham H12 media (Invitrogen) followed by centrifugation at 400g for 10 min at 4°C. MAECs were grown in media described previously.[50]

Generation of Expression Constructs

The GST-tagged recombinant proteins of the full length Noxa (pGEX-Noxa), 5′ or 3′ truncated versions (pGEX-NoxaΔ5′ or pGEX-NoxaΔ3′), C25/51S mutant (pGEX-Noxa-2CS), and C-terminal K35/38/41R mutant (pGEX-Noxa-3KR) were expressed in pGEX-5X-1 Gene Fusion System (GE Health). The constructs were generated by

amplifying the desired coding regions with appropriate mutations using PCR and inserting the products into the BamHI and EcoRI sites of pGEX-5X1 vector. The primers for generating NOXA full-length and truncated constructs were: NOXA (BamHI)- 5′-tcc gga ctc gga tcc cca tgc ct-3′ NOXA (EcoRI)- 5′-ccg tcg act gca gaa ttc tca gg-3′ NOXA-5′deletion (BamHI)-5′-cgg atc ccc caa ccg agc ccc gcg cgg gct cca gc-3′ NOXA-3′deletion (EcoRI) – 5′-cag aat tct cac tgc cgg aag ttc agt ttg tct cc-3′. Primers for generating pGEX-Noxa-2CS were: pGEX-NOXA-BamHI-F (5′-aag gtc gtg gga tcc cca tgc ctg gg-3′), NOXA C25S-F (5′-ctg gaa gtc gag tct gct act caa ctc-3′), NOXA C25S-R (5′-gag ttg agt agc aga ctc gac ttc cag-3′), NOXA-C51S-EcoRI-R (5′-cga ccc ggg aat tct cag gtt cct gag gag aag agt ttg g-3′). After generating products PCR1 and PCR2 using primers pGEX-NOXA-BamHI-F / NOXA C25S-R, and NOXA C25S-F / NOXA-C51S-EcoRI-R, these products were purified and used as the templates to amplify PCR3 product using pGEX-NOXA-BamHI-F and NOXA-C51S-EcoRI-R primers. PCR3 was digested with BamHI+EcoRI, and cloned into pGEX-5X1. pGEX-Noxa-3KR was constructed using the following primers: pGEX-NOXA-BamHI-F, NOXA-K35R-R (5′-ctg ccg gaa gtt cag gcg gtc tcc aaa tct-3′), NOXA-K41R-R (5′-gat atc aga ttc aga agg cgc tgc cgg aag ttc ag-3′), NOXA-K48R-EcoRI-R: (5′-cgg gaa ttc tca ggt tcc tga gca gaa gag gcg gga tat cag att cag-3′). To express Noxa and its mutant proteins in mammalian cells, Noxa-WT, Noxa-2C and Noxa-3KR were sub-cloned into the BamHI and EcoRI sites of pcDβA vector. pcDβA-Noxa-C25S and pcDβA-C51S constructs were generated using pGEX-NOXA-BamHI-F/ NOXA-EcoRI-R (5′-cga ccc ggg aat tct cag gtt cct gag cag aag agt ttg g-3′) to amplify pGEX-Noxa-2C and pGEX-NOXA-BamHI-F / NOXA-C51S-EcoRI-R to amplify Noxa-WT. The PCR products were digested with BamHI+EcoRI and sub-cloned into the pcDβA vector, where expression of cloned sequences is driven by the CMV enhancer. All constructs were verified by sequencing.

Immunofluorescence

Cells were seeded onto 2- or 4-well chamber slides (Labtek), fixed with 3.5% paraformaldehyde, permeabilized with 0.1% Triton X-100, and incubated in blocking buffer (3% BSA, 1% normal goat serum in PBS). After incubation with the relevant primary antibody cells were stained with either anti-rabbit Alexa647 or mouse Alexa555 (Invitrogen), mounted with glass coverslips using Fluoromount-G (Southern Biotech) and immunofluorescence visualized using Axioplan 2 (Carl Zeiss) with a Plan-Aprochromal 63×/1.4 oil objective and a charge-coupled device camera (SensiCam; PCO) using an acquisition and processing software Slidebook 5.0 (Intelligent Imaging Innovation, CO).

GST Pull-down Assays

Expression constructs were transformed into ECOS-21 bacterial cells (Yeastern Biotech) and induced using 1mM IPTG (Sigma) for 4 h at 37°C (GE Health, manufacturer's protocol). Cells were lysed by repeated freeze-thawing and sonication. Expression was determined via Western blot analysis using an anti-Noxa Mouse mAb (114C307, Calbiochem). Fusion proteins were affinity-purified on glutathione-Sepharose beads (Pharmacia) and quantified. For pull-down assays, lysates of non-treated and IFN-γ-treated cells were incubated for 2 h with GST fusion proteins noncovalently immobilized on glutathione-Sepharose beads. Beads were washed in cell lysis buffer (50 mM Tris (pH 7.5), 150 mM NaCl, 0.5% Triton

X-100, 1 mM PMSF, 0.07 trypsin inhibitor units/ml of aprotinin, and 1 μg/ml each of leupeptin, pepstatin, antipain, and chymostatin (Sigma)). Bound proteins were solubilized in sample buffer, resolved by SDS-PAGE, and subjected to anti-HSP27 immunoblotting.

Preparation of Cytoplasmic and Nuclear Extracts

Briefly, cells were lysed in 100 μl lysis buffer (10 mM Tris-HCl, pH8.0; 60 mM KCl; 1 mM EDTA; 1 mM DTT, protease Inhibitors cocktail, 0.5% NP-40), and nuclei centrifuged at 2000g. Nuclear extract was obtained by incubating nuclei in nuclear extraction buffer (20 mM Tris-HCl; 420 mM NaCl; 0.2 mM EDTA; 25% glycerol; 1.5 mM $MgCl_2$; 1 mM DTT and 0.1 mM PMSF) and centrifugation at 10,000g.[15]

Immunoblotting

Western blot analysis was performed as described previously [15]. Briefly, equal amount of proteins were resolved by SDS-PAGE and transferred to PVDF membranes (Immobilon-P, Millipore Corp). Membranes were incubated with optimal concentrations of relevant primary antibody and incubated with horseradish peroxidase (HRP)-conjugated anti-mouse or -rabbit secondary antibody (Sigma), washed 3×5 min in TBS-T and visualized by Western Lightning Plus-ECL according to manufacturer's protocol (Perkin Elmer). The antibodies used were mouse Noxa (114C307) (Calbiochem), rabbit anti-Noxa (FL-54), anti-κBα (C-21) and mouse anti-NF-κB p65 (F-6) (Santa Cruz Biotechnology), rabbit anti-Lamin A/C and mouse HSP27 (Cell Signaling Technology), rabbit anti-p-Ser [15, 78, or 82] HSP27 (Stressgen), anti-K48-linkage Specific Polyubiquitin mAB (Cell Signaling), mouse anti-β-Actin, and anti-β-tubulin (Sigma).

Immunoprecipitation

The Crosslink IP Kit (Thermo Fisher Scientific) was used to cross-link 10 μg of anti-Noxa, anti-NF-κB and anti-κBα (Santa Cruz) or HSP27 (Stressgen) antibodies to Sepharose protein A beads using disuccinmidyl suberate according to manufacturer's protocol. The associated proteins were immunoprecipitated by gentle mixing equal amounts of protein lysates with the antibody-crosslinked beads at 4°C overnight. After 6 washes, bead-bound proteins were eluted and analyzed by immunoblotting.

Retroviral silencing with shRNA

Retroviral silencing vector encoding shHSP27 or shNoxa and the corresponding control vector (shCtrl) were purchased from Origene Technologies, Inc. The suppressing effect of the shRNA was first established in AALEB cells and the subsequent amplification, purification, and packaging of the retroviral particles using Phoenix cells (Orbigen, Inc.) were performed as specified by the manufacturer.

Luciferase assay

A549 /NF-κB-luc cell line (Panomics Corp.) was used to monitor the activity of NF-κB transcription factor in a cell based assay (R/D Biosystems, Minneapolis, MN). Cells were lysed by rocking for 15 min in passive lysis buffer (Promega Corp., Madison, WI) and

luciferase activity was detected with the Luciferase Assay system (Promega) using a Fluoroskan Ascent detector (Labsystems) according to the manufacturer's protocol.

Luminex Cytokine Assay

The cytokines in cell culture media were quantified by Luminex instrument (Luminex Corp.) using Multiplex Fluorescent Bead-Based Luminex Cytokine Assays (EMD Millipore).

MALDI-TOF

To identify interacting proteins, Noxa was immunoprecipitated with antibodies cross-linked to Sepharose protein A beads. The immunoprecipitate was fractionated on a SDS-PAGE and the 32 kDa band along with blank controls excised, eluted, and subjected to tryptic digestion. Samples were dissolved in methanol, mixed at a 1:1 ratio (v/v) with 2,5-dihydrobenzoic acid (20 mg/ml in 70% methanol in water) as matrix. Survey scans were acquired from m/z 500–4,000. Sequence analysis of the tryptic peptides was performed using matrix-assisted laser desorption/ionization time-of-flight mass spectrometry (ABI 4700 MALDI /TOF Mass Spectrometer) running 4000 Series Explorer. Precursors for MS/MS were selected on the basis of signal intensity with up to 20 peptides per spot being chosen for MS/MS analysis. Peptide sequences were identified by searching MASCOT® database using GPS Explorer Version 3.5 software (Applied Biosystems). Both MS and MS/MS spectra were processed by the software. For MS spectra, an S/N threshold of 30 was used, while for MS/MS spectra, a threshold of 20 was used to detect peaks.

Real-time PCR Analysis

Total RNA was isolated from HAECs, MAECs and AALEB cells using RNeasy Micro Kit (QIAGEN). The mRNA levels of Noxa, IL-1β, IL-6, Bcl-2, Bcl-x_L were quantified by ABI HT 7900 Real Time PCR system using TaqMan One-step RT-PCR Gene Expression kit (Life Technologies). The mRNA levels of KC from MAECs were quantified using High Capacity RNA-to-cDNA Kit (Life Technologies) and QuantiTect SYBR Green PCR Kit (QIAGEN).

Statistical Analysis

Grouped results from at least three different experiments were expressed as means ± SEM. Results (grouped by time point and treatment) were analyzed using two-way analysis of variance. In the event that significant main effects were detected ($P < 0.05$), Fisher's least significant difference test was used to differentiate between groups. A P-value of 0.05 was considered to indicate statistical significance. Data were analyzed using statistical analysis software (Statistical Analysis Software Institute).

Supplementary Material

Refer to Web version on PubMed Central for supplementary material.

Acknowledgments

The authors thank Dr. Ram H. Nagaraj for providing HSP27 WT and C137A expression constructs and Lois K. Herrera for technical assistance with Luminex assays and quantification of inflammation in lung tissues. These studies were supported by grants from the National Institutes of Health (HL068111 and ES015482).

References

1. Artis D, Spits H. The biology of innate lymphoid cells. Nature. 2015; 517(7534):293–301. [PubMed: 25592534]
2. Muhl H, Pfeilschifter J. Anti-inflammatory properties of pro-inflammatory interferon-gamma. International immunopharmacology. 2003; 3(9):1247–1255. [PubMed: 12890422]
3. Su X, Yu Y, Zhong Y, Giannopoulou EG, Hu X, Liu H, et al. Interferon-gamma regulates cellular metabolism and mRNA translation to potentiate macrophage activation. Nature immunology. 2015; 16(8):838–849. [PubMed: 26147685]
4. Kelchtermans H, Billiau A, Matthys P. How interferon-gamma keeps autoimmune diseases in check. Trends in immunology. 2008; 29(10):479–486. [PubMed: 18775671]
5. Zheng T, Kang MJ, Crothers K, Zhu Z, Liu W, Lee CG, et al. Role of cathepsin S-dependent epithelial cell apoptosis in IFN-gamma-induced alveolar remodeling and pulmonary emphysema. J Immunol. 2005; 174(12):8106–8115. [PubMed: 15944319]
6. Li XM, Chopra RK, Chou TY, Schofield BH, Wills-Karp M, Huang SK. Mucosal IFN-gamma gene transfer inhibits pulmonary allergic responses in mice. J Immunol. 1996; 157(8):3216–3219. [PubMed: 8871613]
7. Nicoletti F, Di Marco R, Zaccone P, Xiang M, Magro G, Grasso S, et al. Dichotomic effects of IFN-gamma on the development of systemic lupus erythematosus-like syndrome in MRL-lpr / lpr mice. European journal of immunology. 2000; 30(2):438–447. [PubMed: 10671199]
8. Wahl SM, Allen JB, Ohura K, Chenoweth DE, Hand AR. IFN-gamma inhibits inflammatory cell recruitment and the evolution of bacterial cell wall-induced arthritis. J Immunol. 1991; 146(1):95–100. [PubMed: 1898608]
9. Nandi B, Behar SM. Regulation of neutrophils by interferon-gamma limits lung inflammation during tuberculosis infection. The Journal of experimental medicine. 2011; 208(11):2251–2262. [PubMed: 21967766]
10. de Bruin AM, Libregts SF, Valkhof M, Boon L, Touw IP, Nolte MA. IFNgamma induces monopoiesis and inhibits neutrophil development during inflammation. Blood. 2012; 119(6):1543–1554. [PubMed: 22117048]
11. Ohnmacht C, Pullner A, van Rooijen N, Voehringer D. Analysis of eosinophil turnover in vivo reveals their active recruitment to and prolonged survival in the peritoneal cavity. J Immunol. 2007; 179(7):4766–4774. [PubMed: 17878375]
12. Gajewski TF, Fitch FW. Anti-proliferative effect of IFN-gamma in immune regulation. I. IFN-gamma inhibits the proliferation of Th2 but not Th1 murine helper T lymphocyte clones. J Immunol. 1988; 140(12):4245–4252. [PubMed: 2967332]
13. Cooks T, Pateras IS, Tarcic O, Solomon H, Schetter AJ, Wilder S, et al. Mutant p53 prolongs NF-kappaB activation and promotes chronic inflammation and inflammation-associated colorectal cancer. Cancer cell. 2013; 23(5):634–646. [PubMed: 23680148]
14. Shi ZQ, Fischer MJ, De Sanctis GT, Schuyler M, Tesfaigzi Y. IFNg but not Fas mediates reduction of allergen-induced mucous cell metaplasia by inducing apoptosis. J Immunol. 2002; 168:4764–4771. [PubMed: 11971027]
15. Mebratu YA, Dickey BF, Evans C, Tesfaigzi Y. The BH3-only protein Bik/Blk/Nbk inhibits nuclear translocation of activated ERK1/2 to mediate IFNgamma-induced cell death. The Journal of cell biology. 2008; 183(3):429–439. [PubMed: 18981230]
16. Contreras AU, Mebratu Y, Delgado M, Montano G, Hu CA, Ryter SW, et al. Deacetylation of p53 induces autophagy by suppressing Bmf expression. The Journal of cell biology. 2013; 201(3):427–437. [PubMed: 23629966]

17. Villunger A, Michalak EM, Coultas L, Mullauer F, Bock G, Ausserlechner MJ, et al. p53-and drug-induced apoptotic responses mediated by BH3-only proteins puma and noxa. Science. 2003; 302(5647):1036–1038. [PubMed: 14500851]
18. Grespi F, Soratroi C, Krumschnabel G, Sohm B, Ploner C, Geley S, et al. BH3-only protein Bmf mediates apoptosis upon inhibition of CAP-dependent protein synthesis. Cell death and differentiation. 2010; 17(11):1672–1683. [PubMed: 20706276]
19. Ekoff M, Kaufmann T, Engstrom M, Motoyama N, Villunger A, Jonsson JI, et al. The BH3-only protein Puma plays an essential role in cytokine deprivation induced apoptosis of mast cells. Blood. 2007; 110(9):3209–3217. [PubMed: 17634411]
20. Oda E, Ohki R, Murasawa H, Nemoto J, Shibue T, Yamashita T, et al. Noxa, a BH3-only member of the Bcl-2 family and candidate mediator of p53-induced apoptosis. Science. 2000; 288(5468): 1053–1058. [PubMed: 10807576]
21. Ploner C, Kofler R, Villunger A. Noxa: at the tip of the balance between life and death. Oncogene. 2008; 27 Suppl 1:S84–92. [PubMed: 19641509]
22. Kunsch C, Rosen CA. NF-kappa B subunit-specific regulation of the interleukin-8 promoter. Molecular and cellular biology. 1993; 13(10):6137–6146. [PubMed: 8413215]
23. Ozes ON, Mayo LD, Gustin JA, Pfeffer SR, Pfeffer LM, Donner DB. NF-kappaB activation by tumour necrosis factor requires the Akt serine-threonine kinase. Nature. 1999; 401(6748):82–85. [PubMed: 10485710]
24. Karin M. Nuclear factor-kappaB in cancer development and progression. Nature. 2006; 441(7092): 431–436. [PubMed: 16724054]
25. Grice GL, Nathan JA. The recognition of ubiquitinated proteins by the proteasome. Cellular and molecular life sciences : CMLS. 2016; 73(18):3497–3506. [PubMed: 27137187]
26. Alves NL, Derks IA, Berk E, Spijker R, van Lier RA, Eldering E. The Noxa/Mcl-1 axis regulates susceptibility to apoptosis under glucose limitation in dividing T cells. Immunity. 2006; 24(6): 703–716. [PubMed: 16782027]
27. Kim H, Rafiuddin-Shah M, Tu HC, Jeffers JR, Zambetti GP, Hsieh JJ, et al. Hierarchical regulation of mitochondrion-dependent apoptosis by BCL-2 subfamilies. Nature cell biology. 2006; 8(12): 1348–1358. [PubMed: 17115033]
28. Huang L, Min JN, Masters S, Mivechi NF, Moskophidis D. Insights into function and regulation of small heat shock protein 25 (HSPB1) in a mouse model with targeted gene disruption. Genesis. 2007; 45(8):487–501. [PubMed: 17661394]
29. Ermolaeva MA, Michallet MC, Papadopoulou N, Utermohlen O, Kranidioti K, Kollias G, et al. Function of TRADD in tumor necrosis factor receptor 1 signaling and in TRIF-dependent inflammatory responses. Nature immunology. 2008; 9(9):1037–1046. [PubMed: 18641654]
30. Danial NN, Walensky LD, Zhang CY, Choi CS, Fisher JK, Molina AJ, et al. Dual role of proapoptotic BAD in insulin secretion and beta cell survival. Nature medicine. 2008; 14(2):144–153.
31. Yeretssian G, Correa RG, Doiron K, Fitzgerald P, Dillon CP, Green DR, et al. Non-apoptotic role of BID in inflammation and innate immunity. Nature. 2011; 474(7349):96–99. [PubMed: 21552281]
32. Kim JY, Ahn HJ, Ryu JH, Suk K, Park JH. BH3-only protein Noxa is a mediator of hypoxic cell death induced by hypoxia-inducible factor 1alpha. The Journal of experimental medicine. 2004; 199(1):113–124. [PubMed: 14699081]
33. Davis AL, Qiao S, Lesson JL, Rojo de la Vega M, Park SL, Seanez CM, et al. The quinone methide aurin is a heat shock response inducer that causes proteotoxic stress and Noxa-dependent apoptosis in malignant melanoma cells. The Journal of biological chemistry. 2015; 290(3):1623–1638. [PubMed: 25477506]
34. Karim CB, Michel Espinoza-Fonseca L, James ZM, Hanse EA, Gaynes JS, Thomas DD, et al. Structural Mechanism for Regulation of Bcl-2 protein Noxa by phosphorylation. Scientific reports. 2015; 5:14557. [PubMed: 26411306]
35. Verma R, Peters NR, D'Onofrio M, Tochtrop GP, Sakamoto KM, Varadan R, et al. Ubistatins inhibit proteasome-dependent degradation by binding the ubiquitin chain. Science. 2004; 306(5693):117–120. [PubMed: 15459393]

36. Lanneau D, de Thonel A, Maurel S, Didelot C, Garrido C. Apoptosis versus cell differentiation: role of heat shock proteins HSP90, HSP70 and HSP27. Prion. 2007; 1(1):53–60. [PubMed: 19164900]

37. Garrido C. Size matters: of the small HSP27 and its large oligomers. Cell death and differentiation. 2002; 9(5):483–485. [PubMed: 11973606]

38. Andrieu C, Taieb D, Baylot V, Ettinger S, Soubeyran P, De-Thonel A, et al. Heat shock protein 27 confers resistance to androgen ablation and chemotherapy in prostate cancer cells through eIF4E. Oncogene. 2010; 29(13):1883–1896. [PubMed: 20101233]

39. Jia Y, Ransom RF, Shibanuma M, Liu C, Welsh MJ, Smoyer WE. Identification and characterization of hic-5/ARA55 as an hsp27 binding protein. The Journal of biological chemistry. 2001; 276(43):39911–39918. [PubMed: 11546764]

40. Crowe J, Aubareda A, McNamee K, Przybycien PM, Lu X, Williams RO, et al. Heat shock protein B1-deficient mice display impaired wound healing. PloS one. 2013; 8(10):e77383. [PubMed: 24143227]

41. Park KJ, Gaynor RB, Kwak YT. Heat shock protein 27 association with the I kappa B kinase complex regulates tumor necrosis factor alpha-induced NF-kappa B activation. The Journal of biological chemistry. 2003; 278(37):35272–35278. [PubMed: 12829720]

42. Parcellier A, Schmitt E, Gurbuxani S, Seigneurin-Berny D, Pance A, Chantome A, et al. HSP27 is a ubiquitin-binding protein involved in I-kappaBalpha proteasomal degradation. Molecular and cellular biology. 2003; 23(16):5790–5802. [PubMed: 12897149]

43. Hu R, Ouyang Q, Dai A, Tan S, Xiao Z, Tang C. Heat shock protein 27 and cyclophilin A associate with the pathogenesis of COPD. Respirology. 2011; 16(6):983–993. [PubMed: 21585617]

44. Merendino AM, Paul C, Vignola AM, Costa MA, Melis M, Chiappara G, et al. Heat shock protein-27 protects human bronchial epithelial cells against oxidative stress-mediated apoptosis: possible implication in asthma. Cell Stress Chaperones. 2002; 7(3):269–280. [PubMed: 12482203]

45. Straume O, Shimamura T, Lampa MJ, Carretero J, Oyan AM, Jia D, et al. Suppression of heat shock protein 27 induces long-term dormancy in human breast cancer. Proceedings of the National Academy of Sciences of the United States of America. 2012; 109(22):8699–8704. [PubMed: 22589302]

46. Tesfaigzi Y, Fischer MJ, Green FHY, De Sanctis GT, Wilder JA. Bax is crucial for IFNg-induced resolution of allergen-induced mucous cell metaplasia. J Immunol. 2002; 169:5919–5925. [PubMed: 12421976]

47. Lundberg AS, Randell SH, Stewart SA, Elenbaas B, Hartwell KA, Brooks MW, et al. Immortalization and transformation of primary human airway epithelial cells by gene transfer. Oncogene. 2002; 21(29):4577–4586. [PubMed: 12085236]

48. Germain M, Mathai JP, McBride HM, Shore GC. Endoplasmic reticulum BIK initiates DRP1-regulated remodelling of mitochondrial cristae during apoptosis. The EMBO journal. 2005; 24(8): 1546–1556. [PubMed: 15791210]

49. You Y, Richer EJ, Huang T, Brody SL. Growth and differentiation of mouse tracheal epithelial cells: selection of a proliferative population. American journal of physiology Lung cellular and molecular physiology. 2002; 283(6):L1315–1321. [PubMed: 12388377]

50. Mou H, Vinarsky V, Tata PR, Brazauskas K, Choi SH, Crooke AK, et al. Dual SMAD Signaling Inhibition Enables Long-Term Expansion of Diverse Epithelial Basal Cells. Cell stem cell. 2016

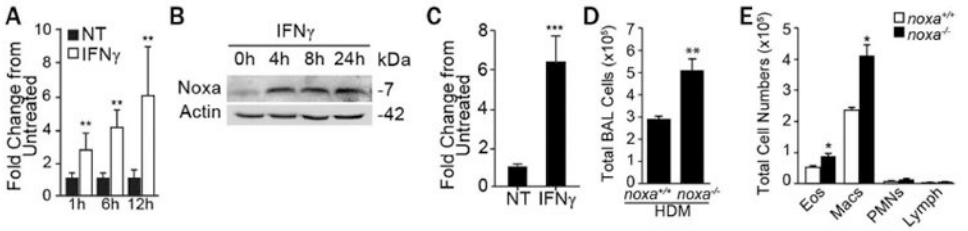

Figure 1. IFN-γ Induces Noxa Expression to inhibit inflammation

(A) AALEB cells treated with IFN-γ or vehicle over 48 h and analyzed for Noxa mRNA by q-PCR. Data represented as the mean ± SEM (n= 3 wells/for each time point and repeated at least 3 times). **(B)** Protein extracts from HAECs treated with IFN-γ or vehicle and Noxa protein levels analyzed by Western blotting (representative of 3 experiments). **(C)** HAECs from 14 individuals treated with 50 ng/ml IFN-γ and analyzed for Noxa mRNA levels by q-PCR. **(D+E)** The *noxa*$^{+/+}$ and *noxa*$^{-/-}$ mice challenged with HDM extracts (50 μg) intranasally in 50 μl saline for 4 days (n=5 mice/group) and the lung inflammatory cells quantified in the bronchoalveolar lavage (BAL) fluid collected 24 h later. BAL cell differentials quantified after staining with Wright Giemsa. The number of total cells **(D)** and eosinophils, macrophages, neutrophils, and lymphocytes **(E)**. Error bars indicate ± SEM, * $P < 0.05$, ** $P < 0.01$, *** $P < 0.001$.

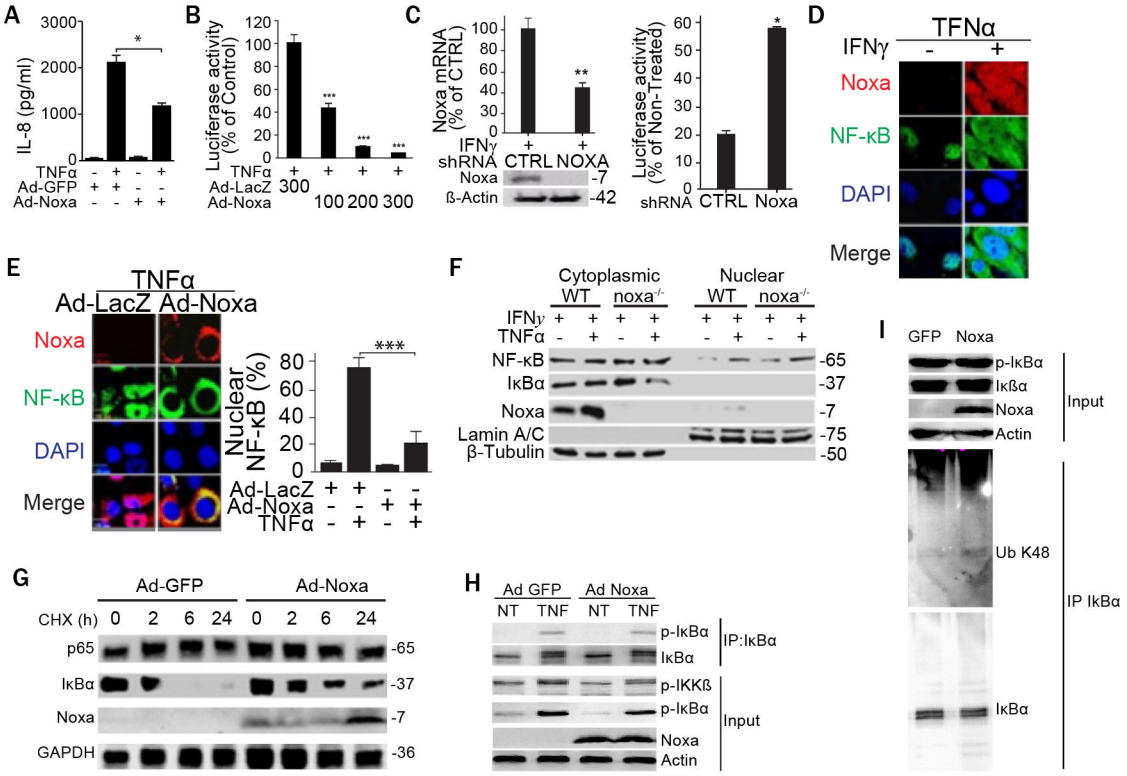

Figure 2. Noxa blocks TNFα-induced NF-κB nuclear translocation and promoter activation by prolonging the half-life of IκBα: (A)

AALEB cells were infected with Ad-Noxa or Ad-GFP (80 MOI) and were treated or left untreated with 20 ng/ml of TNFα for 24 h. Secreted IL-8 was quantified by Luminex assay (n= 3 experiments with 3 wells in each experiment). **(B)** Luciferase activity in A549-Luc cells when either infected with 100, 200 or 300 MOI Ad-Noxa or 300 MOI Ad-LacZ and stimulated with TNFα for 30 min, or **(C)** when the cells were stably transfected with shNoxa or shCtrl and treated with IFN-γ; reduced expression of Noxa mRNA and protein by shNoxa was verified by qRT-PCR and Western blotting. **(D)** AALEB cells treated with IFN-γ (50 ng/ml) or vehicle and 24 h later with TNFα for 30 min. Cells immunostained with antibodies to NF-κB and Noxa and counterstained with Hoechst 33342. **(E)** Immunostaining with antibodies to NF-κB and Noxa of AALEB cells infected with Ad-Noxa or Ad-LacZ treated with TNFα for 30 min; percentage of cells with nuclear NF-κB. Error bar indicates ± SEM (n=3 independent experiments with 3 wells in each experiment). * $P < 0.05$, ** $P < 0.01$, *** $P<0.001$. **(F)** Cytosolic and nuclear extracts from *noxa*$^{+/+}$ and *noxa*$^{-/-}$ MAECs treated with IFN-γ and TNFα and analyzed by Western blotting. **(G)** AALEB cells infected with Ad-Noxa and Ad-GFP and treated with cyclohexamide. Extracts probed for NF-κB, IκB, Noxa, and GAPDH. **(H+I)** AALEB cells infected with Ad-GFP or Ad-Noxa, treated with 10 μM MG-132 and 30 min later with vehicle or 10 ng/ml TNFα; cells harvested 10 min later and extracts immunoprecipitated with anti-IκBα antibodies. **(H)** The levels of p-IκBα and Noxa levels were determined with the respective controls in input and immunoprecipitates. **(I)** Levels of p-IκBα and Noxa levels in the input and IκBα and K48 chain-linked ubiquitin of IκBα were determined in the immunoprecipitates. Western blots are representative of 3 different experiments.

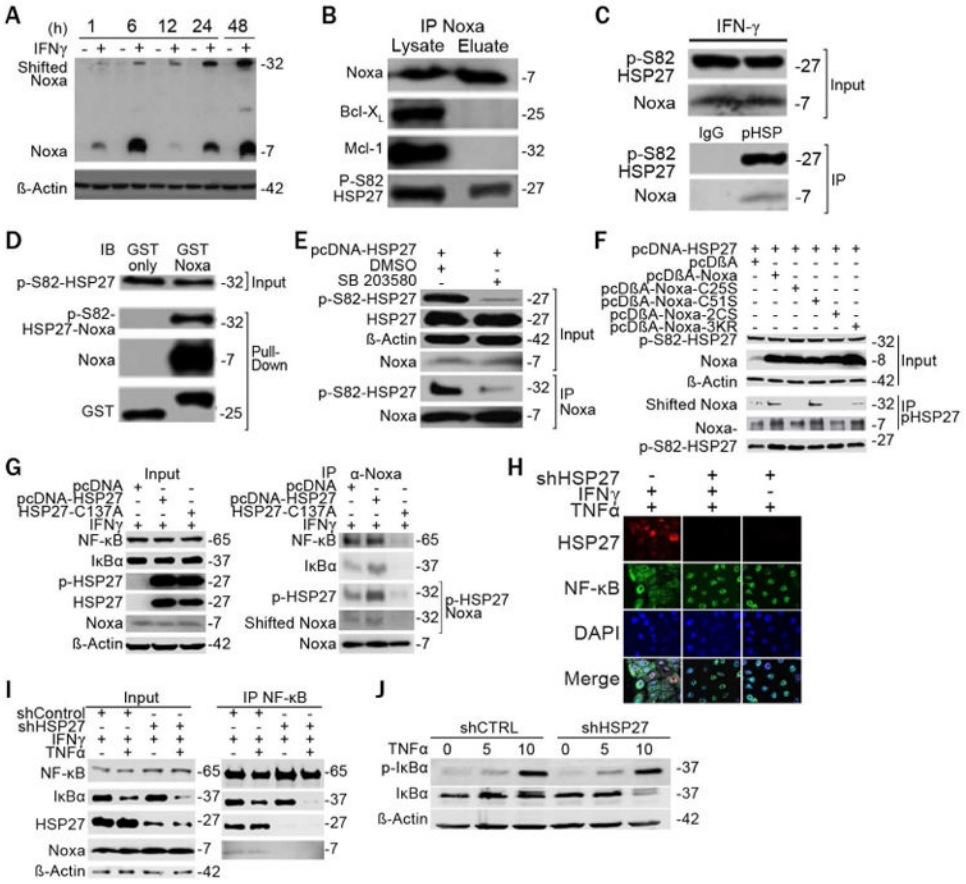

Figure 3. The cross-linking of Noxa and p-HSP27 is essential for blocking NF-κB activation

(A) Noxa (6 kDa) and a 32 kDa cross-reactive protein detected by Noxa antibodies in IFN-γ-treated AALEB cells. **(B)** Immunoprecipitates using anti-Noxa antibody from IFN-γ-treated cells analyzed by immunoblotting. **(C)** Immunoprecipitates using IgG as control or p-S_{82}HSP27 antibodies from IFN-γ-treated AALEB cells analyzed by immunoblotting with antibodies to p-S_{82}HSP27 and Noxa. **(D)** GST or GST-Noxa proteins bound to glutathione-sepharose beads used to pull down proteins from AALEB cell lysates and analyzed by Western blotting. **(E)** Protein extracts from AALEB cells transfected with HSP27 expression vector and treated with the p38MAPK inhibitor, SB203580, were immunoprecipitated using anti-Noxa antibodies. **(F)** HSP27 was co-transfected with Noxa, NoxaC25S, NoxaC51S, Noxa2CS, or Noxa3KR and immunoprecipitated using anti-p-S_{82}HSP27. **(G)** Immunoprecipitates using Noxa antibodies from lysates of HEK293T cells expressing $HSP27^{WT}$, $HSP27C^{137A}$, and Noxa analyzed by Western blotting. **(H)** Immunofluorescence of shCtrl and shHSP27 cells treated with IFN-γ and/or TNFα or vehicle using antibodies to NF-κB and p-S_{82}HSP27 and counterstained with Hoechst 33342. **(I)** Immunoprecipitates using anti-NF-κB from shCtrl and shHSP27 cells treated with IFN-γ and TNFα or vehicle and analyzed by immunoblotting. **(J)** Lysates from shCtrl and shHSP27 cells pre-treated with CHX and 10 ng/ml TNFα analyzed by Western blotting. All Western blots are representative of at least 3 different experiments.

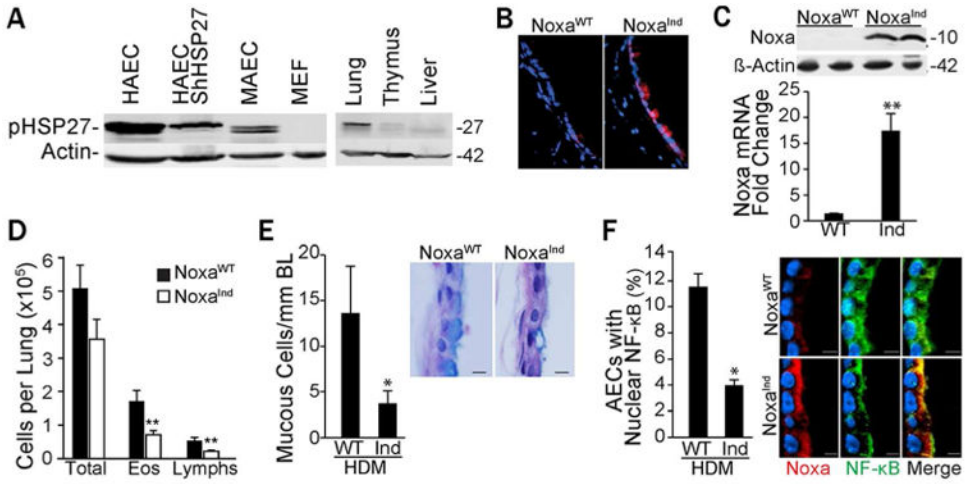

Figure 4. Inducible transgenic expression of Noxa in airway epithelial cells protects mice from inflammation: (A)

pHSP27 levels in HAECs, MAECs, MEFs and in murine lung, thymus, and liver tissues tested for by Western blotting. **(B)** Immunostaining with Noxa antibodies of tissue sections from the left lungs of Noxa^{Ind} and Noxa^{WT} littermates. **(C)** Noxa protein and mRNA levels in the right lungs analyzed by Western blottin and q-PCR, respectively. **(D)** Noxa^{Ind} and Noxa^{WT} mice were challenged with HDM extracts intranasally for 5 days, fed dox diet for 2 days, and lungs lavaged 24 h later (n=8 mice/group). The number of total cells, eosinophils and lymphocytes were quantified. **(E)** Mucous cell numbers per mm basal lamina (BL) were quantified using VisioMorph system on Alcian blue/hematoxylin and eosin (AB/H&E) stained sections (n=8/group). Representative images of AB/H&E-stained airway epithelium from Noxa^{Ind} and Noxa^{WT} mice. **(F)** Co-immunostaining with Noxa (red) and NF-κB (green) antibodies of airway epithelium from Noxa^{Ind} and Noxa^{WT} littermates following HDM challenge and dox-diet. Quantification of percentage airway epithelial cells with nuclear NF-κB in Noxa^{Ind} and Noxa^{WT} mice exposed to HDM (n=5/group). Error bars indicate ± SEM * $P < 0.05$,

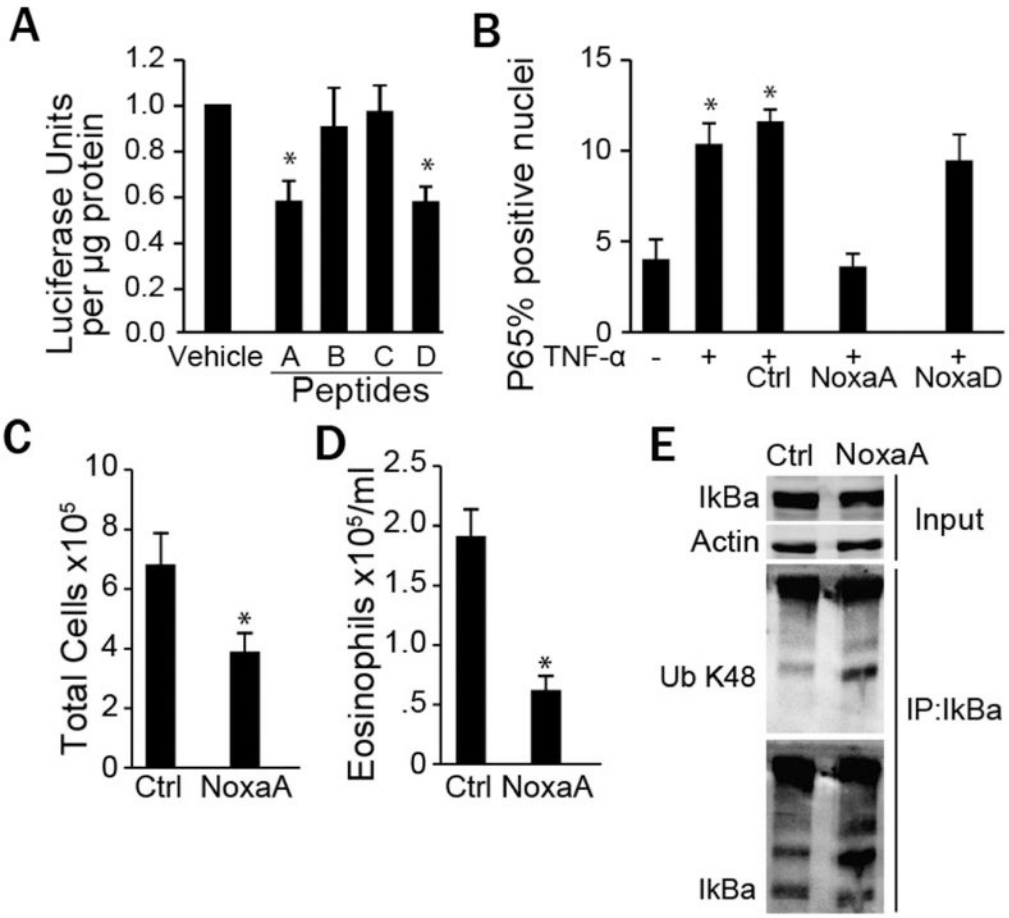

Figure 5. N-terminal peptide of Noxa is sufficient to prolong IκBα half-life and block inflammation

(A) Luciferase activity in A549-Luc cells treated with vehicle or peptides A, B, C, and D at 50 nM concentration. **(B)** Nuclear localization of NF-κB (p65) following treatment of *noxa*$^{-/-}$ MAECs with 0 or 10 ng/ml TNFα in the presence of TAT-Ctrl, and peptides A or D. **(C + D)** C57Bl/6 mice exposed to 50 µg house dust mite for 5 consecutive days and instilled with 10 µM each of TAT-Ctrl or peptide A on days 6 and 7. On day 8, the numbers of total inflammatory cells (C) and eosinophils **(D)** were assessed in the BAL fluid. Error bar indicates ± SEM (in 2 separate experiments with minimum of 4 mice/group each). * $P <$ 0.05. **(E)** AALEB cells were treated with TAT-Ctrl or peptide A and 24 h later treated with TNFα for 10 min. Immunoprecipitates with anti-IκBα antibodies were analyzed for levels of IκBα and K48 chain linked ubiquitin of IκBα and IκBα and β-actin in the input. Western blots are representative of 3 different experiments.